Coupling and noise in the circadian clock synchronization

Alessio Franci[1]✉, Marco Arieli Herrera-Valdez[1]✉ Miguel Lara-Aparicio[1]✉, Pablo Padilla-Longoria[2]✉,
[1] Facultad de Ciencias,
Universidad Nacional Autónoma de México, Mexico.
[2] Instituto de Investigación en Matemáticas Aplicadas y Sistemas,
Universidad Nacional Autónoma de México, Mexico.
✉ afranci@ciencias.unam.mx, marcoh@ciencias.unam.mx, mla@ciencias.unam.mx, pablo@mym.iimas.unam.mx

Keywords: Circadian rhythm, synchronization, nonlinear oscillators, Fokker-Planck, Hopf bifurcation.

Abstract

The general purpose of this paper is to build up on our understanding of the basic mathematical principles that underlie the emergence of biological rhythms, in particular, the circadian clock. To do so, we study the role that the coupling strength and noise play in the synchronization of a system of nonlinear, linearly coupled oscillators. First, we study a deterministic version of the model to find plausible regions in the parameter space for which synchronization is observed. Second, we focus on studying how noise and coupling interact in determining the synchronized behavior. To do so, we leverage the Fokker-Planck equation associated with the system. The basic mechanisms behind the generation of oscillations and the emergence of synchrony that we describe here can be used as a guide to further study coupled oscillations in biophysical nonlinear models.

1 Introduction

The study of circadian rhythms has been a subject of great interest for a long time. However, the majority of the first studies were mainly based on observations in plants [1], and mathematical modeling of biological rhythms was then at a very early stage [2–4]. There are two milestones in the study of circadian rhythms from a mathematical perspective, namely, the association of circadian rhythms to the existence of a limit cycle [5] and Arthur Winfree's master book entitled "The Geometry of Biological Time" [6]. Related to the work of Kalmus, several mathematical models of circadian rhythm were presented in a Symposium on Biological Rhythms carried out at Cold Spring Harbor in the United States of America in 1960 [7–9]. Among these works, one of the most important entitled "Shock excited system as models for biological rhythms" was presented by Kalmus, a biologist, and Wigglesworth, a mathematician [5]. In this paper the authors associated a limit cycle to a circadian rhythm, using a hydraulic system as analogy. Lots of other important works on circadian rhythms were presented in this symposium, but the work of Kalmus and Wigglesworth was the crucial one in establishing a better mathematical formalism for the study of circadian rhythms. Although many researchers followed the theoretical path proposed by Kalmus and Wigglesworth, the mathematical study of circadian rhythms was finally established by Arthur Winfree (biologist and mathematician), who introduced topology for the description of several aspects of circadian rhythms. Lara-Aparicio *et al.* have worked on both mathematical modeling and experimental characterizations of different properties of circadian rhythms since 1993, when they first published an article on the ontogeny of circadian rhythm in the crayfish [10]. In their work, they built a mathematical model that phenomenologically captures a series of experimental results involving the synchronization of electro-retinogram activity in crayfish [11–13]. The model was constructed by coupling two van der Pol oscillators [14] represented by state vectors $\mathbf{x} = (x_1, x_2, x_3)^T$ and $\mathbf{y} = (y_1, y_2, y_3)^T$. The coupled system from [10] is given by

$$\dot{\mathbf{x}} = F(\mathbf{x}; k, c, r), \quad \dot{\mathbf{y}} = F(\mathbf{y}; l, C, R) \tag{1}$$

The parameters k and l represent the frequency of the oscillator; r and R are functions that represent the radii of the limit cycles, and c and C are also functions that represent the first coordinate of the center

PeerJ Preprints | https://doi.org/10.7287/peerj.preprints.26447v1 | CC BY 4.0 Open Access | rec: 19 Jan 2018, publ: 19 Jan 2018

of the limit cycle. The system is setup such that one oscillator driving the behavior of the other oscillator, but not vice-versa. The coupling terms are c and r, which are functions of $\mathbf{x}$ and $\mathbf{y}$, in the equations for the first oscillator $\mathbf{x}$. The driving oscillator induces an Andronov-Hopf bifurcation in the driven oscillator and regulates its frequency.

The model in equations (1) allows analytical approaches, and it makes it possible to answer questions referring to the ontogeny of the circadian rhythm in crayfish from the childhood to adult stages. The behavior of this phenomenological model simulates, explains, and has suggested new biological experiments. For instance, a hypothesis about the existence of a hormone which was experimentally detected was generated from the model. The model also allowed Lara-Aparicio *et al.* to study synchronization of circadian rhythms with external signals like day and night light [15]. The studying of basic principles has enabled researchers to conjecture that circadian rhythms can result from coupling systems of cells, each one oscillating with an ultradian oscillation [16–18]. In particular, Lara-Aparicio *et al.* have studied the theme of synchronization among cells through the following system of nonlinear equations [19],

$$\ddot{x}_i = f_i\left(x_i, \dot{x}_i\right) + \sum_{j \neq i} a_{ij}(x_j - x_i) \tag{2}$$

with

$$f_i\left(x_i, \dot{x}_i\right) = \mu\left(1 - x_i^2\right)\dot{x}_i \tag{3}$$

where x_i, i=1,2,3,4, represents the ith oscillator, with the classical van der Pol non-linear damping for the terms f_i responsible for the oscillatory dynamics.

In the present paper, we extend the work in [10] and [19] by analyzing two qualitative mathematical models, each capturing a different level of organization in the ontogeny of circadian rhythms. The first model produces neuronal dynamics at the cellular level. Then, using graph theoretical methods and center manifold theory, we show that synchronous oscillations appear via a Hopf-Bifurcation in a population of pacemaker neurons. To model gap junction coupling between the neurons, the coupling is assumed to be diffusive. The bifurcation parameter models the development stage of the neurons. We further explore the phenomenon of oscillator death: although the single neurons are endogenously oscillating for sufficiently large bifurcation parameter, the population oscillation dies for sufficiently large coupling, which suggests that the weak coupling hypothesis must be satisfied for robust synchronous oscillations to occur. In the case of all-to-all coupling, we provide necessary conditions for oscillator death to occur and leave the derivation of sufficient conditions to future works. The second model captures the interconnection of various circadian pacemaker populations. Each population is assumed to be an endogenous oscillator and the coupling is assumed to be linear. Using linear stochastic analysis and under the assumption that the population oscillations are synchronized, we derive a scalar Fokker-Plank equation. Under this assumption, we derive an estimate of the synchronization frequency as a function of the intrinsic frequencies of the oscillators, their coupling strength, and the topology of the network. The model is shown to capture an important feature of circadian rhythm ontogeny: the emergence of low frequency (circadian) oscillations from coupled high frequency (ultradian) oscillators, originally studied in [19]. Future work will aim at deriving conditions on the intrinsic frequencies, the coupling strength, and the network topology, that ensure synchronization of the the population oscillations.

2 Global synchronization of clock neurons

We consider a network of oscillators on a directed graph $\mathcal{G}$ with N vertices. The network topology is codified in the adjacency matrix $A = [a_{ij}]_{i,j=1}^{N}$, where $a_{ij} \geq 0$. If oscillator i receives signals from oscillator j, then the graph has an arrow from oscillator j to oscillator i, and $a_{ij} > 0$. The dynamics for

PeerJ Preprints | https://doi.org/10.7287/peerj.preprints.26447v1 | CC BY 4.0 Open Access | rec: 19 Jan 2018, publ: 19 Jan 2018

each oscillator are assumed to satisfy the following coupled oscillator dynamics

$$\dot{x}_i = y_i + \mu \sum_{j=1}^{N} a_{ij}(x_j - x_i) \tag{4a}$$

$$\dot{y}_i = \left(\lambda - x_i^2 - \frac{y_i^2}{\omega^2}\right) y_i - \omega_i^2 x_i \tag{4b}$$

The parameter $\lambda \in \mathbb{R}$ determines the endogenous behavior of each oscillator, and $\mu \geq 0$ represents a generic coupling strength. In the absence of coupling the oscillator dynamics reduces to the modified van der Pol equation

$$\ddot{x} = \left(\lambda - x_i^2 - \frac{y_i^2}{\omega^2}\right) \dot{x} - \omega_i^2 x.$$

For $\lambda < 0$ the nonlinear dissipation coefficient $-\left(\lambda - x^2 - \frac{y^2}{\omega_i^2}\right)$ is always positive which leads to damped oscillations. For $\lambda > 0$ the dissipation coefficient becomes negative close to the origin, which leads to sustained oscillations via a Hopf bifurcation. Given the specific form of the equation, a generic trajectory belonging to the family of periodic orbits born at the Hopf bifurcation has the form

$$\sqrt{\lambda}(\cos(\omega_i t + \theta_0), \sin(\omega_i t + \theta_0)), \tag{5}$$

where the θ_0 is the initial phase.

We start by recalling some basic graph-theoretical definitions and facts.

Definition 2.1 *The Laplacian matrix $L = [L_{ij} : i, j = 1, ..., n]$ for the graph $\mathcal{G}$ is such that $L_{ij} = -a_{ij}$ if $i \neq j$, $L_{ii} = \sum_{j=1}^{N} a_{ij}$.*

Note that $L1_N = 0$. That is, the vector of ones is always a right null eigenvector of L and zero is always an eigenvalue of L.

Definition 2.2 *The interconnection graph is said to be connected if for each pair of nodes in the graph, there exists a connection between them.*

Lemma 2.3 *A graph is connected if and only zero is a simple eigenvalue of the Laplacian [20].*

Definition 2.4 *A graph is balanced if $\sum_{j=1}^{N} a_{ij} = \sum_{j=1}^{N} a_{ji}$ for all i.*

Obviously, symmetric graphs (i.e., satisfying $a_{ij} = a_{ji}$) are balanced. The converse is not true. Consider, for instance, a directed ring.

The global behavior of the system (4) for $\lambda < 0$, $\mu \geq 0$, for a generic graph is characterized by the next theorem (Figure 1).

Theorem 2.5 *Assume that the graph $\mathcal{G}$ is balanced and that $\omega_i = \omega_j = \omega$ for all $i, j = 1, \ldots, N$. If $\lambda < 0$, then the origin is globally asymptotically stable and locally exponentially stable for all $\mu \geq 0$.*

Proof. We consider the quadratic Lyapunov function

$$V(x, y) = \sum_{i=1}^{N} (x_i^2 + y_i^2/\omega^2).$$

The derivative of V along the trajectories of the system (4) gives

$$\dot{V} = \sum_{i=1}^{N} \left(2x_i\dot{x}_i + 2y_i\dot{y}_i/\omega^2\right) \tag{6}$$

PeerJ Preprints | https://doi.org/10.7287/peerj.preprints.26447v1 | CC BY 4.0 Open Access | rec: 19 Jan 2018, publ: 19 Jan 2018

which after substitution of the derivatives $\dot{x}_i$ and $\dot{y}_i$, can be bounded from above as follows

$$
\begin{aligned}
&= \sum_{i=1}^{N} \left(2x_i y_i - 2\mu x_i \sum_{j=1}^{N} a_{ij}(x_i - x_j) - 2y_i \frac{\omega^2 x_i}{\omega^2} + 2\frac{y_i}{\omega^2} \left(\lambda - x_i^2 - \frac{y_i^2}{\omega^2} \right) y_i \right) \\
&\leq 2\frac{\lambda}{\omega^2} \sum_{i=1}^{N} y_i^2 - 2\mu \sum_{i,j=1}^{N} x_i a_{ij}(x_i - x_j) \\
&= 2\frac{\lambda}{\omega^2} \sum_{i=1}^{N} y_i^2 - 2\mu \sum_{i,j=1}^{N} a_{ij}(x_i^2 - x_j x_i) \\
&= 2\frac{\lambda}{\omega^2} \sum_{i=1}^{N} y_i^2 - 2\mu \sum_{i,j=1}^{N} a_{ij}(x_i^2/2 - x_j x_i + x_i^2/2)
\end{aligned}
$$

To show that the last term is negative definite, we use the balanced interconnection hypothesis. Let $d_j = \sum_{i=1}^{N} a_{ij} = \sum_{i=1}^{N} a_{ji}$. We have

$$
\sum_{i,j=1}^{N} a_{ij} x_j = \sum_{j=1}^{N} d_j x_j = \sum_{i=1}^{N} d_i x_i = \sum_{i,j=1}^{N} a_{ij} x_i.
$$

As a consequence,

$$
\dot{V} \leq \frac{\lambda}{\omega^2} \sum_{i=1}^{N} y_i^2 - 2\mu \sum_{i,j=1}^{N} a_{ij}(x_i - x_j)^2 \leq \frac{\lambda}{\omega^2} \sum_{i=1}^{N} y_i^2.
$$

Then the global part of statement follows by LaSalle invariance principle [21]. The local part follows by observing that for $\lambda < 0$ the linearization of model (4) at the origin is non-singular and therefore asymptotic stability of the origin implies that all eigenvalues have negative real part. □

Remark 2.6 *Because exponentially stability implies robustness to small perturbations, Theorem 2.5 remains true for small heterogeneity in the natural frequencies.*

Figure 1, top, shows that for $\lambda < 0$ model (4) exhibits exponentially damped oscillations toward the origin.

Next we show that, at $\lambda = 0$ and identical natural frequencies model (4) undergoes a supercritical Hopf bifurcation inside the consensus space

$$
\mathcal{C} = \{(x, y) \in \mathbb{R}^{2N} : x_i = x_j,\, y_i = y_j,\, \forall i, j = 1, \ldots, N\},
$$

provided the graph is strongly connected. The linearization of the system (4) is given by

$$
J = \begin{bmatrix} -\mu L & I_N \\ -\omega^2 I_N & \lambda I_N \end{bmatrix}, \tag{7}
$$

where I_N is the N-dimensional identity matrix and L is the network Laplacian defined in Definition (2.1). Let 1_N be the N-dimensional vector of ones. Given a (complex) vector $\nu = (v, w)$ in the consensus space $\mathcal{C}$, that is, $v = a1_N$ and $w = b1_N$ for some $a, b \in \mathbb{C}$, the eigenvalue problem for the jacobian

PeerJ Preprints | https://doi.org/10.7287/peerj.preprints.26447v1 | CC BY 4.0 Open Access | rec: 19 Jan 2018, publ: 19 Jan 2018

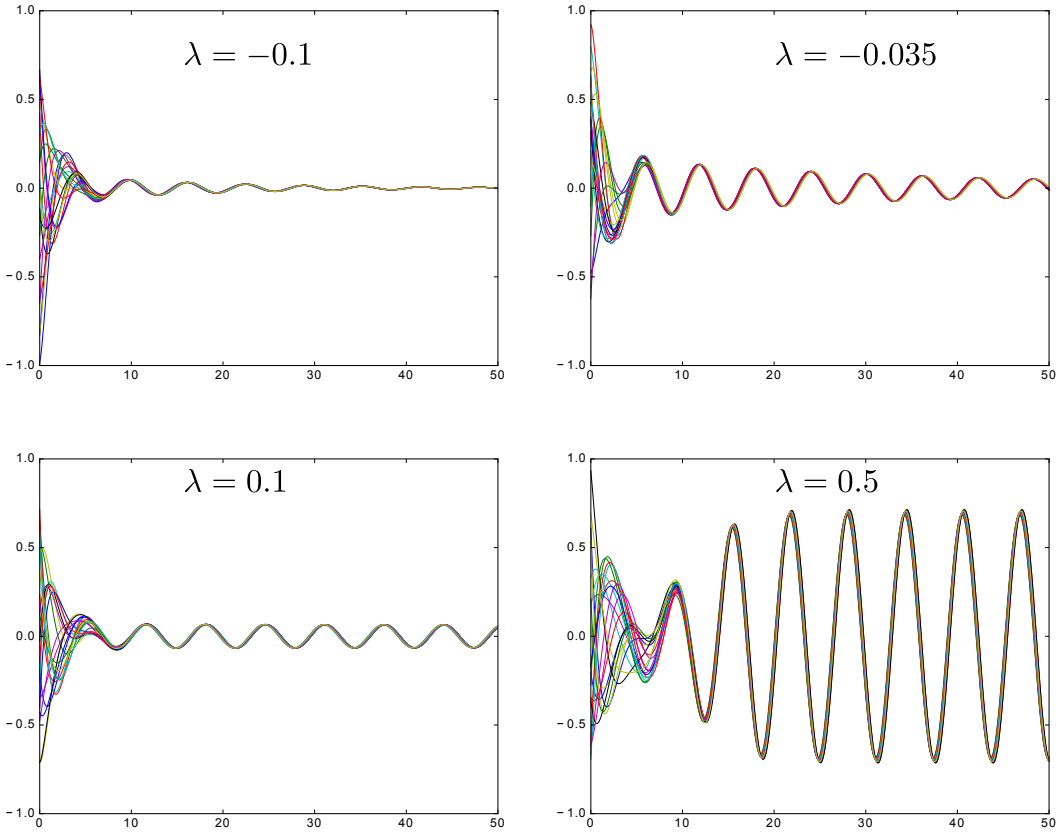

Figure 1: Transition between global asymptotic stability and synchronous oscillation via Hopf bifurcation in system (4) for $\mu = 0.05$, $N = 20$, natural frequencies uniformly distributed in the interval $[0.9, 1.1]$ and varying λ. The interconnection topology is all-to-all.

matrix (7), restricted to the consensus space, takes the form

$$\begin{aligned} J\nu &= J \begin{bmatrix} a1_N \\ b1_N \end{bmatrix} \\ &= \begin{bmatrix} -\mu L a1_N + b1_N \\ -\omega^2 a + \lambda b1_N \end{bmatrix} \\ &= \begin{bmatrix} b1_N \\ (-\omega^2 a + \lambda b)1_N \end{bmatrix} \\ &= \xi \begin{bmatrix} a1_N \\ b1_N \end{bmatrix} \end{aligned}$$

where ξ is a (complex) eigenvalue. In the third equality we used the fact that 1_N is a right null eigenvector of L. The last equality implies that $\nu \in \mathcal{C}$ is an eigenvector of J with eigenvalue ξ if and only if its

PeerJ Preprints | https://doi.org/10.7287/peerj.preprints.26447v1 | CC BY 4.0 Open Access | rec: 19 Jan 2018, publ: 19 Jan 2018

components a and b satisfy

$$\begin{bmatrix} 0 & 1 \\ -\omega^2 & \lambda \end{bmatrix} \begin{bmatrix} a \\ b \end{bmatrix} = \xi \begin{bmatrix} a \\ b \end{bmatrix}. \tag{8}$$

We can now easily solve (8) to obtain the eigenvalues/eigenvectors pairs

$$\xi_{\pm}(\lambda) = \frac{\lambda}{2} \pm \frac{1}{2}\sqrt{\lambda^2 - 4\omega^2}, \quad \begin{bmatrix} a_{\pm} \\ b_{\pm} \end{bmatrix} = \begin{bmatrix} \frac{1}{\omega^2}(\lambda - \xi_{\pm}) \\ 1 \end{bmatrix} \tag{9}$$

For $\lambda = 0$ we got two purely imaginary eigenvalues which correspond to a supercritical Hopf bifurcation of model (4) inside the consensus space, as summarized in the following theorem and illustrated in Figure 1 bottom.

Theorem 2.7 *For almost all balanced, strongly connected interconnection topologies the following holds. For all $\mu > 0$, the system (4) undergoes a supercritical Hopf bifurcation at $\lambda = 0$ with center manifold given by the consensus space $\mathcal{C}$. Moreover, the family of periodic solutions born at the Hopf bifurcation are exponentially asymptotically stable and correspond to synchronous oscillations of the oscillator network.*

Proof. By Theorem 2.5 the origin is locally exponentially stable for $\lambda < 0$. We further observe that, if the interconnection topology is strongly connected, then by Lemma 2.3 zero is a simple eigenvalue of L and therefore no either eigenvalue of J satisfies the eigenvalue problem defined by (4). It then follows by the center manifold theorem [22] and equation (9), that the system (4) possesses a two-dimensional center manifold $\mathcal{W}^c$ that is tangent to the consensus space $\mathcal{C}$ for $\lambda = 0$. Moreover, this center manifold is exponentially attractive. By the Hopf bifurcation theorem [23], equation (9) also implies that the system (4) undergoes a supercritical Hopf bifurcation inside $\mathcal{W}^c$ when λ crosses zero from negative to positive. By direct substitution inside the model equations, we see that along a generic member of the family of periodic orbits born at the Hopf bifurcation, oscillators are synchronously oscillating with each oscillator orbit given by equation (5). □

Remark 2.8 *Because Hopf bifurcation is codimension-zero (in the sense of [24]), it is persistent under to small perturbations, which ensures that Theorem 2.7 remains true for small heterogeneity in the natural frequencies.*

2.1 Oscillator death and multi-stability for stronger coupling

We now explore the phenomenon of "oscillator death", induced in model (4) by too a strong coupling. We restrict our attention to the all-to-all coupling case, i.e., $a_{ij} = 1$ for all $i \neq j$. For $\lambda > 0$ and μ sufficiently small the synchronous oscillations born at Hopf bifurcation proved in Theorem 2.7 attract all trajectory. However, as illustrated in Figure 2, increasing μ leads to the appearance of a family of steady states that attract part of the trajectories, although the synchronous periodic orbits remain locally exponentially stable. Indeed, depending on the initial conditions, some trajectories converge to the synchronous oscillations: the system is *multistable*. In the following we will provide geometric insights, without formal proof, about the mechanisms underlying oscillator death and multi-stability in model (4).

We start by observing that the oscillator death state is characterized by the presence of two oscillator clusters. Inside each clusters, oscillators converge to the same steady state. To analyze the appearance of oscillator death steady-states we can use this observation and simplify the model equations by assuming that $(x_i, y_i) = (x_1, y_1)$ for all $i = 1, \ldots, N_1$ and $(x_i, y_i) = (x_2, y_2)$ for all $i = 1, \ldots, N_2$, where $N_1, N_2 < N$, $N_1 + N_2 = N$, are the cluster sizes. The pairs (x_1, y_1) and (x_2, y_2) define the cluster states.

PeerJ Preprints | https://doi.org/10.7287/peerj.preprints.26447v1 | CC BY 4.0 Open Access | rec: 19 Jan 2018, publ: 19 Jan 2018

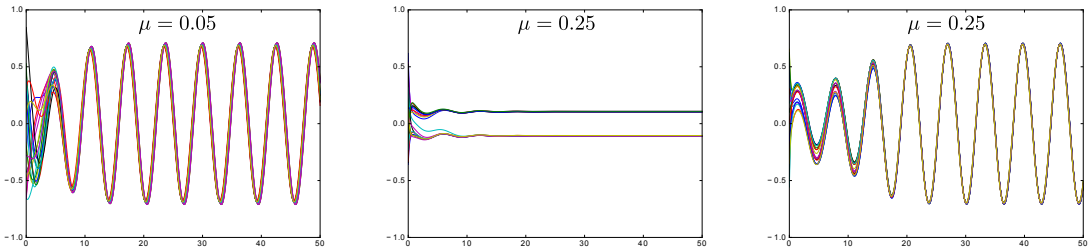

Figure 2: Emergence of oscillator death in model (4) for $\lambda = 0.5$, $N = 20$, natural frequencies uniformly distributed in the interval $[0.9, 1.1]$ and varying μ. The interconnection topology is all-to-all. Note that for the same value of $\mu = 0.25$ both oscillatory and oscillator death states are possible.

The cluster state dynamics can easily be derived and read

$$\dot{x}_1 = y_1 + \mu N_2(x_2 - x_1), \tag{10a}$$

$$\dot{y}_1 = -\omega^2 x_1 + \left(\lambda - x_1^2 - \frac{y_1^2}{\omega^2}\right) y_1, \tag{10b}$$

$$\dot{x}_2 = y_2 + \mu N_1(x_1 - x_2), \tag{10c}$$

$$\dot{y}_2 = -\omega^2 x_2 + \left(\lambda - x_2^2 - \frac{y_2^2}{\omega^2}\right) y_2. \tag{10d}$$

Each cluster state dynamics has the form

$$\dot{x} = y + \mu N_j(x_j - x), \tag{11a}$$

$$\dot{y} = -\omega^2 x + \left(\lambda - x^2 - \frac{y^2}{\omega^2}\right) y, \tag{11b}$$

where N_j is the other cluster size and x_j the other cluster state. A sufficient condition for the appearance of multiple steady states is that there must exist values of x_j for which model (11) possesses multiple steady-states. This condition can easily be verified by analyzing the intersection of the nullclines of model (11). They are drawn if Figure 3 for $x_j = 0$, $\omega = 1.0$, $N = 20$ and $N_1 = N_2 = N/2$, $\lambda = 0.5$ and various values of μ.

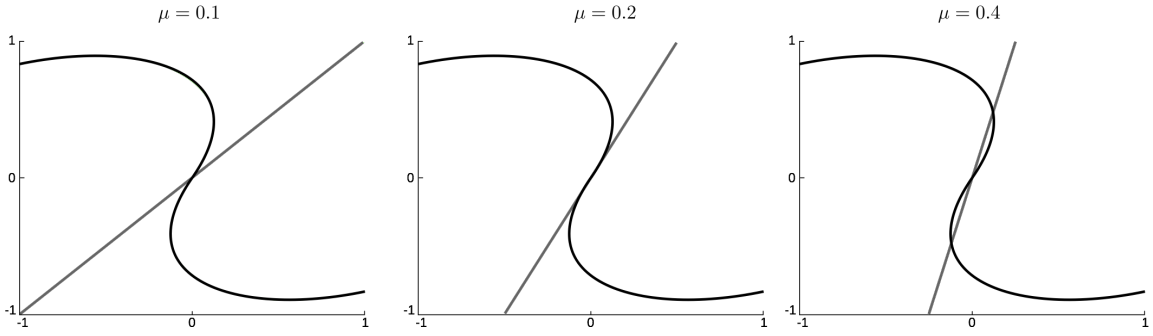

Figure 3: Nullclines of the cluster state dynamics for incresing values of μ

PeerJ Preprints | https://doi.org/10.7287/peerj.preprints.26447v1 | CC BY 4.0 Open Access | rec: 19 Jan 2018, publ: 19 Jan 2018

If the coupling strength is too small the origin is the only steady state. This steady state is unstable and all trajectories are attracted toward the synchronous periodic orbit. However, for larger μ new steady states appear. The critical value of μ at which the new steady-state appear can be found by computing the slope of the nullclines at the origin. The slope of the x-nullcline is evidently μN_j. The slope of the x-nullcline can be computed by implicit differentiation and is given by $\frac{\omega^2}{\lambda}$. Multiple steady-states appear if $\mu > \frac{\omega^2}{N_j \lambda}$ as verified by the numerical simulations in Figure 2.

3 Synchronization and frequency modulation in coupled circadian pacemakers

In this section we present an alternative approach to study synchronization under the influence of noise using the Fokker-Planck equation (FPE). A related work in the context of populations of synchronized neurons is given in [25]. Introducing noise in the equation is natural from the biological perspective. However, even in the absence of noise, the introduction of random perturbations will allow us, by letting the their amplitude go to zero, to extract information about the deterministic system. The basic idea is that the FPE equation considerably simplifies under the assumption of synchronization and it reduces to an equation in two variables. This enables us to make approximations in order to investigate the dependence of the synchronization frequency on the frequencies of the coupled oscillators, and the different coupling parameters. We divide this section in two parts. In the first we consider a simple deterministic system in which the effect of coupling can be understood. In the second part, we randomly perturb a more general version of the previous model and show that the FP equation provides an approximation for the syncrhonization frequency and some insights on the effect of noise. Let us then consider a system similar to the one already studied

$$\ddot{x}_i = -\omega^2 x_i + \nu \left(1 - \left(x_i^2 + \frac{\dot{x}_i^2}{\omega^2}\right)\right) \dot{x}_i + \mu \sum_{j=1}^{N} a_{ij} x_j, \quad i = 1, \ldots, N, \tag{12}$$

Notice that $x(t) = sin(\omega t)$ is still a solution for the uncoupled system ($\mu = 0$), independently of the value of ν.

If we linearize the equation and take $\nu << 1$, we can neglect the contribution of the disipative term. The resulting linear system is

$$\ddot{x}_i = -(\omega^2 - \mu A_i) x_i,$$

where $A_i = \sum_{j=1}^{N} a_{ij} x_j, \quad i = 1, \ldots, N$. If all the $a_{ij} = 1$, corresponding to a fully connected network of oscillators, the previous system is consistently reduces to the equation

$$\ddot{x} = -(\omega^2 - \mu(N-1))x,$$

if we assume that a synchronized regime is established. This provides an estimate for the synchronization frequency of

$$\Omega_{sync} = \sqrt{\omega^2 - \mu(N-1)}.$$

Moreover, this reduction suggests that synchronized oscillatory behavior takes place for sufficiently small μ. That is, when

$$\omega^2 - \mu(N-1) > 0,$$

Otherwise, exponentially large growth can be expected. Notice that unless the a_{ij} are equal, the previous reasoning is not consistent and no conclusion can be drawn. We claim that introducing random

PeerJ Preprints | https://doi.org/10.7287/peerj.preprints.26447v1 | CC BY 4.0 Open Access | rec: 19 Jan 2018, publ: 19 Jan 2018

perturbations and using the FP equation allows us to circumvent this difficulty and analyze the general case. This is the content of what follows. First of all, we write the system in the form

$$\begin{aligned}\dot{x}_i &= y_i \\ \dot{y}_i &= f_i(x_i, y_i) + \mu \sum_{j=1}^{N} a_{ij} x_j, \quad i = 1, \ldots, N.\end{aligned}$$

Notice that in the linearized regime, anologous to the reasoning for small ν in the previous example, we might naturally assume that

$$f_i(x_i, y_i) \approx -\omega_i^2.$$

Perturbing the equation with Brownian noise we have

$$\begin{aligned}dx_i &= y_i\, dt + \sqrt{2\varepsilon}\, dW_{i1} \\ dy_i &= \left[-\omega_i^2 x_i + \mu \sum_{j=1}^{N} a_{ij} x_j \right] dt + \sqrt{2\varepsilon}\, dW_{i2}, \quad i = 1, \ldots, N,\end{aligned}$$

where the W_{ij} are uncorrelated Brownian motions. The probability density, $u(x_1, ..., x_n, y_1, ..., y_n, t)$ of the system being in the state $x_1, ..., x_n, y_1, ..., y_n$ at time t satisfies the FP equation

$$\frac{\partial u}{\partial t} = \varepsilon \Delta u + \nabla (F(x, y) u),$$

where F is the vector field determined by the right hand side of the stochastic system. Looking for stationary solutions, i.e. $u_t = 0$ and explicitely substituting F in terms of x and y, the equation becomes

$$\varepsilon \Delta u + \sum_i \left(y_i u_{x_i} + (-\omega^2 x_i + \mu \sum_{j \neq i} a_{ij} x_j) u_{y_i} \right) = 0. \tag{13}$$

If we use the synchronization condition $x_1 = x_2 = ... = x_n$ and $y_1 = y_2 = ... = y_n$ we obtain the equation

$$\varepsilon \Delta + n y u_x + (-\sum_i \omega_i^2 + \mu \sum_{i,j} a_{ij}) x u_y = 0.$$

If we let

$$b = \sum_i \omega_i^2 - \mu \sum_{i,j} a_{ij},$$

we can write the equation (13) as

$$\varepsilon \Delta + n y u_x - b x u_y = 0.$$

Assuming ε is small, it is reasonable to expect that the probability u will concentrate around the characteristic curves of the first order equation

$$n y u_x - b x u_y = 0,$$

that are solutions to the system

$$\begin{aligned}\dot{x} &= n y, \\ \dot{y}_i &= b x.\end{aligned}$$

By taking the scalar product with the vector $(x/n, y/b)$ we obtain the relation

$$\dot{x} \frac{x}{n} + \dot{y} \frac{y}{b} = 0,$$

PeerJ Preprints | https://doi.org/10.7287/peerj.preprints.26447v1 | CC BY 4.0 Open Access | rec: 19 Jan 2018, publ: 19 Jan 2018

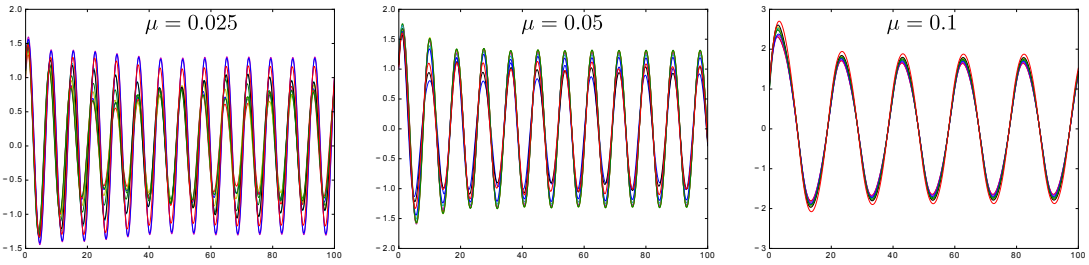

Figure 4: Synchronization and modulation of the synchronization frequency via coupling strength in model (12), for $N = 10$, natural frequencies uniformly distributed in the interval $[0.95, 1.05]$, all-to-all coupling and varying μ.

or equivalently,

$$\frac{x^2}{n} + \frac{y^2}{b} = constant,$$

which defines the characteristic curves as ellipses. In turn, interpreting these as curves in the phase portrait, the resulting solutions would correspond to periodic trajectories with frequency

$$\Omega_{sync}^2 = -\frac{b}{n} = \frac{(\sum_i \omega_i^2 - \mu \sum_{i,j} a_{ij})}{n}. \tag{14}$$

Formula (14) provides an estimate for the synchronization frequency in terms of the original frequencies and the coupling parameters. Importantly, it shows that the synchronization frequency decreases with the coupling strength: couple ultradian oscillation can give rise to circadian oscillations. This illustrated in Figure 4.

4 Discussion

We have described, through basic geometrical analysis, the relationship between the dissipation coefficient, an intrinsic property of the oscillators we study, and the coupling strength μ in a strongly connected network of nonlinear oscillators. Our analysis predicts the emergence of sustained oscillations for increasing values of the parameter λ in the system, only for a limited range of coupling strengths. It is reasonable to conjecture from this result, that there is a functional limit in the coupling strength for oscillating tissues in nature. Also, in the last section, we have also derived an estimation for the synchronization frequency in terms of the original frequencies and the coupling parameters (equation (14)). We believe that these results constitute predictions that, although possibly difficult to test experimentally, would be worth verifying.

The results we have presented thus far emphasize the importance of simple mathematical models in understanding pathological situations where undesirable synchronization appears (Parkinson's disease [26, 27], epilepsy [28, 29]). The other way around, it is also of potential importance to unravel mechanisms underlying the disappearance of coordinated oscillatory regimes. In a future publication, we plan to formally justify our estimations, and further, integrate the analysis of oscillations in the cellular and network levels of biological organization, to build up on our understanding of coupling oscillators at the tissue level. Two important extensions of the current models that we are studying are, the full characterization in higher codimension of the bifurcation structures of the system (4), and also, replacements of the

PeerJ Preprints | https://doi.org/10.7287/peerj.preprints.26447v1 | CC BY 4.0 Open Access | rec: 19 Jan 2018, publ: 19 Jan 2018

van der Pol dynamics with biophysical models of excitable cells [30]. This last extension may prove useful to explain possible compensatory mechanisms that take place during the beginning of a pathology [31].

Acknowledgements. The authors would like to thank Beatriz Fuentes-Pardo for her input in discussions about the modeling and its connections with the experimental work she has done. The authors would also like to thank Carolina Barriga-Montoya for her work on the Fokker-Planck equations and her support with the modeling. This research has been supported by DGAPA-PAPIIT(UNAM) grant IA105518.

References

[1] Robert C Bünsow. The circadian rhythm of photoperiodic responsiveness in kalanchoe. In *Cold Spring Harbor Symposia on Quantitative Biology*, volume 25, pages 257–260. Cold Spring Harbor Laboratory Press, 1960.

[2] Balth Pol. Biological rhythms considered as relaxation oscillations. *Journal of Internal Medicine*, 103(S108):76–88, 1940.

[3] DA Sholl. Regularities in growth curves, including rhythms and allometry. *Dynamics of growth processes*, 1954.

[4] T Pavlidis, WF Zimmerman, and J Osborn. A mathematical model for the temperature effects on circadian rhythms. *Journal of theoretical biology*, 18(2):210–221, 1968.

[5] Hans Kalmus and LA Wigglesworth. Shock excited systems as models for biological rhythms. In *Cold Spring Harbor symposia on quantitative biology*, volume 25, pages 211–216. Cold Spring Harbor Laboratory Press, 1960.

[6] Arthur T Winfree. *The geometry of biological time*, volume 12. Springer Science & Business Media, 2001.

[7] Karl Klotter. Theoretical analysis of some biological models. In *Cold Spring Harbor symposia on quantitative biology*, volume 25, pages 189–196. Cold Spring Harbor Laboratory Press, 1960.

[8] Karl Klotter. General properties of oscillating systems. In *Cold Spring Harbor symposia on quantitative biology*, volume 25, pages 185–187. Cold Spring Harbor Laboratory Press, 1960.

[9] Beatrice M Sweeney. The photosynthetic rhythm in single cells of gonyaulax polyedra. In *Cold Spring Harbor symposia on quantitative biology*, volume 25, pages 145–148. Cold Spring Harbor Laboratory Press, 1960.

[10] Miguel Lara-Aparicio, Santiago López de Medrano, Beatriz Fuentes-Pardo, and Enrique Moreno-Sáenz. A qualitative mathematical model of the ontogeny of a circadian rhythm in crayfish. *Bulletin of mathematical biology*, 55(1):97–110, 1993.

[11] Ma Luisa Fanjul-Moles, Enrique Moreno-Sáenz, Natalia Villalobos-Hiriart, and Beatriz Fuentes-Pardo. Erg circadian rhythm in the course of ontogeny in crayfish. *Comparative Biochemistry and Physiology Part A: Physiology*, 88(2):213–219, 1987.

[12] Maria Luisa Fanjul-Moles, Manuel Miranda-Anaya, and Beatriz Fuentes-Pardo. Effect of monochromatic light upon the erg crcadian rhythm during ontogeny in crayfish (procambarus clarkii). *Comparative Biochemistry and Physiology Part A: Physiology*, 102(1):99–106, 1992.

[13] Beatriz Fuentes-Pardo, María Luisa Fanjul-Moles, and Enrique Moreno-Sáenz. Synchronization by light of the erg circadian rhythm during ontogeny in the crayfish. *Biological Rhythm Research*, 23(2):81–91, 1992.

[14] Balth Van der Pol. On “relaxation-oscillations”. *The London, Edinburgh, and Dublin Philosophical Magazine and Journal of Science*, 2(11):978–992, 1926.

PeerJ Preprints | https://doi.org/10.7287/peerj.preprints.26447v1 | CC BY 4.0 Open Access | rec: 19 Jan 2018, publ: 19 Jan 2018

[15] Beatriz Fuentes-Pardo, Miguel Lara-Aparicio, and Santiago López de Medrano. Perturbation of a circadian rhythm by single and periodic signals and its mathematical simulation. *Bulletin of Mathematical Biology*, 57(2):175–189, 1995.

[16] Harold B Dowse, Jeffrey C Hall, and John M Ringo. Circadian and ultradian rhythms in *period* mutants of *Drosophila melanogaster*. *Behavior genetics*, 17(1):19–35, 1987.

[17] Albert Goldbeter. From ultradian biochemical oscillations to circadian rhythms. In *Membranes and Circadian Rythms*, pages 67–93. Springer, 1996.

[18] David Lloyd and Ernest L Rossi. *Ultradian rhythms in life processes: An inquiry into fundamental principles of chronobiology and psychobiology*. Springer Science & Business Media, 2012.

[19] Carolina Barriga-Montoya, Pablo Padilla-Longoria, Miguel Lara-Aparicio, and Beatriz Fuentes-Pardo. Ultradian rhythms underlying the dynamics of the circadian pacemaker. In *Aspects of Pacemakers-Functions and Interactions in Cardiac and Non-Cardiac Indications*. InTech, 2011.

[20] Rafig Agaev and Pavel Chebotarev. On the spectra of nonsymmetric laplacian matrices. *Linear Algebra and its Applications*, 399:157–168, 2005.

[21] Joseph P La Salle. An invariance principle in the theory of stability, differential equations and dynamical systems. *"Proceedings of the International Symposium, Puerto Rico."*, pages 277–286, 1967.

[22] John Guckenheimer and Philip Holmes. Local bifurcations. In *Nonlinear oscillations, dynamical systems, and bifurcations of vector fields*, pages 117–165. Springer, 1983.

[23] Brian D Hassard, Nicholas D Kazarinoff, and Y-H Wan. *Theory and applications of Hopf bifurcation*, volume 41. CUP Archive, 1981.

[24] M. Golubitsky, I. Stewart, and D.G. Schaeffer. *Singularities and Groups in Bifurcation Theory*, volume 1. Springer-Verlag, 1985.

[25] Xianfa Jiao and Rubin Wang. Synchronous firing patterns of neuronal population with excitatory and inhibitory connections. *International Journal of Non-Linear Mechanics*, 45(6):647–651, 2010.

[26] Constance Hammond, Hagai Bergman, and Peter Brown. Pathological synchronization in parkinson's disease: networks, models and treatments. *Trends in neurosciences*, 30(7):357–364, 2007.

[27] Alfons Schnitzler and Joachim Gross. Normal and pathological oscillatory communication in the brain. *Nature reviews neuroscience*, 6(4):285–296, 2005.

[28] Jerome Engel Jr, Anatol Bragin, Richard Staba, and Istvan Mody. High-frequency oscillations: What is normal and what is not? *Epilepsia*, 50(4):598–604, 2009.

[29] José Luis Perez Velazquez and Peter L Carlen. Gap junctions, synchrony and seizures. *Trends in neurosciences*, 23(2):68–74, 2000.

[30] Marco A Herrera-Valdez, Erin C McKiernan, Sandra D Berger, Stefanie Ryglewski, Carsten Duch, and Sharon Crook. Relating ion channel expression, bifurcation structure, and diverse firing patterns in a model of an identified motor neuron. *Journal of computational neuroscience*, 34(2):211–229, 2013.

[31] Erin C McKiernan. A genetic manipulation of motor neuron excitability does not alter locomotor output in drosophila larvae. Technical report, PeerJ PrePrints, 2015.

PeerJ Preprints | https://doi.org/10.7287/peerj.preprints.26447v1 | CC BY 4.0 Open Access | rec: 19 Jan 2018, publ: 19 Jan 2018